

Novel Framework to Integrate Real-Time MR-Guided EP Data with T1 Mapping-Based Computational Heart Models

Sebastian Ferguson¹, Maxime Sermesant², Samuel Oduneye^{1,3},
Sophie Giffard-Roisin², Michael Truong^{1,4}, Labonny Biswas¹,
Nicholas Ayache², Graham Wright^{1,3}, and Mihaela Pop^{1,3}(✉)

¹ Sunnybrook Research Institute, Toronto, Canada
mihaela.pop@utoronto.ca

² Inria - Asclepios Project, Sophia Antipolis, France

³ Medical Biophysics, University of Toronto, Toronto, Canada

⁴ Kings College London, London, UK

Abstract. Real-time MRI-guided electrophysiology (EP) interventions hold the potential to replace conventional X-ray guided procedures aimed to eliminate potentially lethal scar-related arrhythmia. Furthermore, although cardiac MR can provide excellent structural information (i.e., anatomy and scar), these catheter-based procedures have limited electrical information due to sparse electrical maps recorded from endocardial surfaces. In this paper, we propose a novel framework to augment such sparse electrical maps with 3D transmural electrical wave propagation obtained non-invasively using computer modelling. First, we performed real-time MR-guided EP studies using a preclinical pig model (i.e., in 1 healthy and 2 chronically infarcted animals). Specifically, the MR scans employed 2D T1-mapping ($1 \times 1 \times 5$ mm spatial resolution) based on a multi-contrast late enhancement method. For the EP studies we used an MR-compatible system (*Imricor*). Second, the stacks of resulting segmented images were used to build 3D heart models with various zones (i.e., healthy, scar and gray zone). Lastly, the 3D heart models were coupled with simple monodomain reaction-diffusion equations (e.g. eikonal and Aliev-Panfilov). Our simulations showed that these mathematical formalisms are advantageous due to fast computations, allowing us to predict the electrical wave propagation through dense LV meshes (e.g. >100 K elements, element size ~ 1.5 mm) in <3 min on a consumer computer. Overall, preliminary results demonstrated that the 3D MCLE-based models predicted close activation times and patterns compared to our measured EP maps, while also providing 3D transmural information and a precise location of the infarction. Future work will focus on calibrating directly (in near real-time) T1-based personalized heart models from electrical maps obtained during real-time MR-guided EP mapping procedures.

Keywords: Cardiac MRI · Modelling · Electrophysiology · Histopathology

1 Introduction

Ventricular tachycardia (VT), a dangerous arrhythmia, is a major cause of sudden cardiac death in patients with structural disease such as myocardial infarction (MI) [1]. In VT, an abnormal electrical wave propagates around unexcitable scars and through viable channels of reduced functionality [2]. The structural characteristics of infarcted areas are evaluated in the clinics using MR imaging, which has excellent soft tissue contrast. In addition, the changes in electrical properties due to collagenous scar development are identified in the electrophysiology (EP) lab typically under X-ray fluoroscopy, using catheter-based systems (e.g. CARTO, NOGA, Ensite). During the EP study, clinicians aim to thermally ablate the “viable channels” (i.e., the VT substrate where the foci reside). These channels are often found in the peri-infarct area and consist in a mixture of viable and non-viable myocytes. Unfortunately, the success rate of the VT ablations is currently low [1–3] due to various limitations of the EP systems (i.e., sparse electrical maps, surface data, exposure to high X-ray dose during long procedures, invasiveness of VT inducibility test, etc.).

To improve the mapping and VT ablation procedures, many centers fuse contrast-enhanced MR and EP data [4], but currently there is a clear need to further reduce: (a) the total procedure time associated with a typical MR study followed by conventional EP study, and (b) the errors between the location of scar/channels identified in MR and EP data. Thus, an attractive alternative is the use of real-time MR-guided EP systems, which employ MR-compatible catheters. Such systems have been recently implemented in several research centers in the world, with pre-/clinical feasibility studies yielding promising results [5, 6]. Notable, the MR-guided EP mapping systems do not use ionizing radiation and produce significantly lower location errors (~ 3 mm) compared to CARTO system [3].

However, despite considerable efforts and the development of complex systems, two major limitations remain the sparsity of electrical points along with the lack of transmural electrical information (since the electrical maps are recorded only from the endocardial and/or epicardial surfaces). To overcome this limitation, one can use *computational modelling* [7]. This powerful non-invasive tool can be combined with structural information extracted from cardiac MRI to build 3D anatomical models that can be used to predict the abnormal propagation of electrical impulse in the presence of non-conductive scars and to simulate the generation of VT waves looping around dense scars. We have previously used such computational tools by employing 3D MRI-based heart models (histologically validated) obtained from high-resolution *ex vivo* diffusion tensor images of explanted porcine hearts. Some of our heart models were previously personalized from surfacic EP data (i.e., maps of activation times) recorded via x-ray-guided EP systems [8].

In this work, we propose a novel preclinical framework that integrates real-time MR-guided EP data with computerized 3D models of healthy/infarcted hearts. Notable, for scar imaging we used a high-resolution T1 mapping method, recently validated using quantitative histology [10]. This gave us confidence that our 3D heart models (integrating three zones: scar, healthy tissue and channels) are anatomically accurate. We then dissected the propagation of electrical wave through the heart using fast

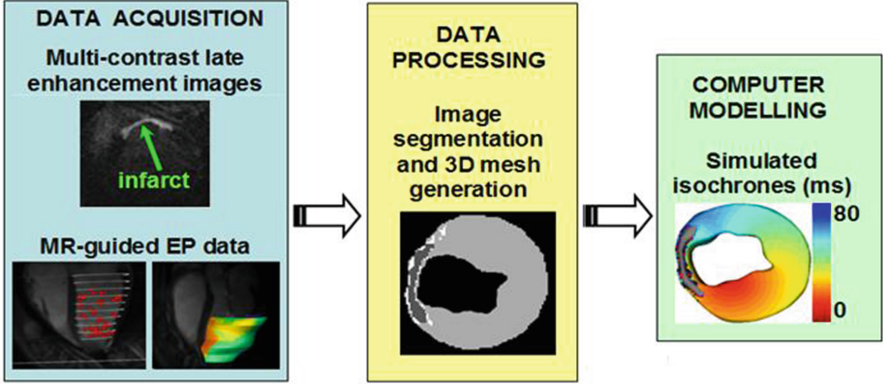


Fig. 1. Diagram of the workflow (see text for more details)

computer models. A simplified diagram of the workflow illustrating various components of the framework is included in Fig. 1.

2 Materials and Methods

2.1 Animal Preparation

In this paper we included results from three MR-EP studies performed in a pre-clinical animal model (i.e., one healthy swine and two swine with chronically infarcted hearts). All interventional procedures received approval from Sunnybrook Research Institute. The methodology of generating myocardial infarction was previously described [8]. Briefly, in this current work, the left ascending artery (LAD) was occluded by a balloon catheter for ~ 90 min, followed by balloon retraction and tissue reperfusion in order to create a heterogeneous infarction that mimicked typical pathological characteristics of MI in humans.

The infarcted animals were allowed to heal for approximately 5–6 weeks prior to the MR-EP studies and to develop chronic fibrosis. By this time point, a dense collagenous scar (i.e., fibrosis) had replaced dead myocytes in the infarct core, while a mixture of viable and non-viable collagen fibrils was found in the peri-infarct. This was confirmed by a collagen-sensitive histological stain as in our previous studies [8].

2.2 Real-Time MR-Guided EP Studies and Data Processing

All MR-EP studies were performed using a 1.5 GE MR scanner. For MR imaging of the heart anatomy we used a cine SSFP sequence, while for scar detection we used our T1 mapping method based on a 2D multi-contrast late enhancement (MCLE) pulse sequence, as previously described [9]. Both types of MR images were acquired using a $1 \times 1 \times 5$ mm spatial resolution.

Our real-time MR-EP system consisted of 8.5 Fr catheters MR-compatible and a prototype EP Recording System (Bridge™, Imricor Medical Systems). We recorded MR signals, tracking data, and intracardiac electrograms (EGMs) from the catheter tip. The MR images acquired for roadmaps were sent to an in-house developed visualization software, Vurtigo (www.vurtigo.ca). Vurtigo also received real-time tracking data and converted them into MR position coordinates for fusion with EP data. Notably, MR and MR-guided EP data are co-registered (by default).

The EGM waveforms gathered from the tip of the catheters were used in conjunction with the catheter coordinates to produce endocardial activation maps. This was achieved by placing a reference catheter on the septum of the RV, and a mapping catheter in the LV. Our system simultaneously recorded the two EGMs and the coordinates of the tracking coils in the catheters. By holding the mapping catheter at one point, we were able to associate a section of the EGMs with a particular coordinate in the endocardium.

The activation time at each of these points was measured manually in Vurtigo by comparing the reference and mapping EGMs. For this, we used a caliper (Fig. 2a) that measured the delay between two peaks in the signals. Example of EGM waveforms from the tip of catheters inserted in RV (for pacing) and LV (for mapping), are shown in Fig. 2b.

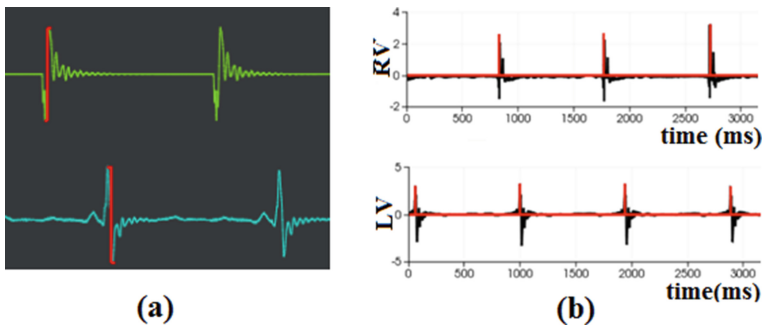


Fig. 2. Electrocardiograms recorded with the Imricor catheter and visualized in Vurtigo: (a) the caliper (in red) measures egm amplitude; and (b) example of recordings from RV and LV under pacing at 400 ms. (Color figure online)

Figure 3a shows an example of fused MR-EP data that was obtained in one infarcted pig. The endocardial contours (drawn in white) were semi-automatically detected in the prior cine SSFP images. The resulting co-registered fused MR data with the EP isochronal map is shown in Fig. 3b. Note that for the color map, early activation/depolarization times are in red and late local activation times in blue. The EGMs were further used to construct endocardial activation maps (i.e., isochrones of depolarization times). The activation maps were recorded from the endocardium of the LV, either in sinus rhythm or under pacing conditions (i.e., at 400 ms, with the pacing catheter placed in the right ventricle, RV, touching the septum).

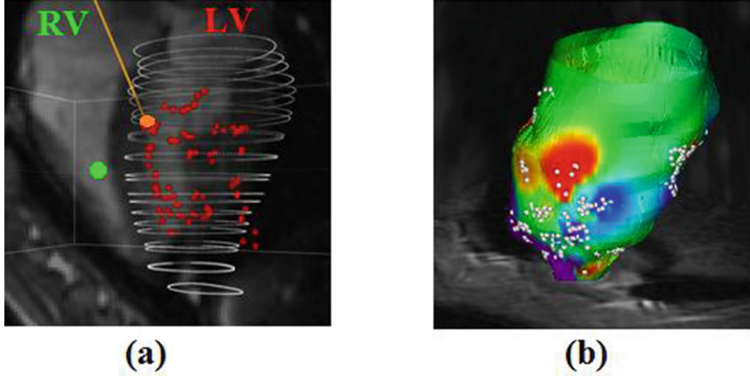


Fig. 3. Visualization of real-time MR-guided EP data in an infarcted pig heart: (a) co-registered MR-EP data; and (b) fused MR image with interpolated isochronal EP map.

For infarcted cases, the MCLE images were used to extract the steady-state and $T1^*$ maps, which were used as an input to a fuzzy-logic segmentation algorithm [9], which is a robust algorithm to cluster infarct core, peri-infarct (grey zone, GZ, where the arrhythmia substrate resides) and healthy pixels.

2.3 Mesh Generation

We generated 3D volumetric LV meshes of sufficiently high density (i.e., between 100–300 K elements, with mean element size approximately 1–1.5 mm), to capture accurately the wave propagation in the peri-infarct areas. All anatomical meshes were constructed using CGAL libraries (www.cgal.org) and Inria tools, from the stacks of segmented 2D MCLE images for infarcted pigs, and from cine SSFP images for the healthy case, respectively.

All 3D meshes integrated synthetic fiber directions generated using rule-based methods that obey analytical equations [10]. For the tissue properties corresponding to the key model parameters, we assigned a different *electrical conductivity value* per each zone (i.e., healthy tissue, slow-conductive GZ and non-conductive scar) to mimic the electrophysiological properties of chronic infarct (see below).

2.4 Computational Modelling

The 3D MCLE-based heart models were further used for simulations. Specifically, we simulated the electrical wave propagation through the heart using two fast mono-domain macroscopic formalism. We then compared the models' output (i.e., isochronal maps) and computational times (tractability) between them and also against the measured isochronal maps. Both mathematical models have a reaction-diffusion term.

The Aliev-Panfilov (A-P) model solves for the action potential (V) and recovery term (r) as described in the reaction-diffusion equations [11, 12]:

$$\frac{\partial V}{\partial t} = \nabla \cdot (D \nabla V) - kV(V - a)(V - 1) - rV \quad (1)$$

$$\frac{\partial r}{\partial t} = -(\varepsilon + \frac{\mu_1 r}{\mu_2 + V})(kV(V - a - 1) + r) \quad (2)$$

where a tunes the action potential duration and k corresponds to the recovery phase. This simplified model accounts for tissue anisotropy (i.e., fiber directions) via the diffusion tensor D , where d is the ‘bulk’ electrical conductivity of tissue. A reduced value of d results in a slow wave propagation, as per the relation between the speed (i.e., conduction velocity) c and d :

$$c = \sqrt{2 \cdot k \cdot d(0.5 - a)} \quad (3)$$

The Eikonal (EK) model is the fastest existing model. This fast model computes only the wave front propagation (i.e., the depolarization phase T_d of the electrical wave) based on the anisotropic Eikonal equation [13]:

$$c^2 (\nabla T_d^t D \nabla T_d) = 1 \quad (4)$$

where the c is the local speed of the wave and D is the diffusion tensor as in the A-P model described above.

Note that in both computational models, we worked with the following value for speed: $c = 30$ cm/s in the GZ (which is a value reduced by 50% compared to c healthy tissue 60 cm/s). We also assigned $c = 0$ in the dense core (which is non-conductive). In both models (A-P and EK) the anisotropy ratio was set to 1:3 (to account for the anisotropic propagation of the electrical wave in transverse vs. longitudinal direction of the fiber).

For all Finite Element simulations, we used a 4,096(1x) MB machine with an Intel® Core™ i3-2310 M processor, 640 GB HD, NVIDIA® GeForce® 315 M graphic adapter.

3 Results and Discussion

Figures 4a–c show exemplary results from the construction of the 3D anatomical model from one of the infarcted hearts, with the scar in the territory of the left anterior descending artery (LAD). From the stack of 2D segmented MCLE images we obtained an interpolated 3D anatomical heart model, which integrated the three types of tissue (GZ, healthy zone and dense scar). The synthetic fibers generated using rule-based methods rotated from -70° to $+70^\circ$ (from endocardium to epicardium), were integrated into the 3D mesh by assigning the fiber directions at each vertex (see example in Fig. 4d).

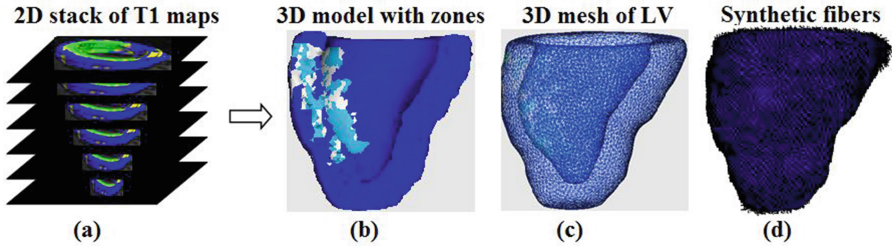


Fig. 4. Construction of the T1-based heart model for one infarcted heart: (a) stack of 2D segmented T1 maps; (b–c) corresponding 3D model and tetrahedral mesh (CGAL); and (d) rule-based synthetic fibers. Notable, the 3D model has three zones: healthy (dark blue), GZ (white) and dense scar (light blue) resulted from segmenting MCLE images. (Color figure online)

Figure 5 presents simulation results obtained for the healthy heart. The outputs of the both EK and A-P models were compared with the recorded endocardial EP map (which was projected onto the endocardial surface of the mesh). Overall, we observed a close correspondence between simulated and measured isochronal maps, as illustrated in Fig. 5-*top*. The A-P model yielded a slightly better match of activation pattern with and a smaller absolute error (8 ms) compared with the measured map, while the simulated isochrones by the EK model lead to a larger absolute (12 ms). Figure 5-*bottom* shows a qualitative comparison of epicardial isochrones (simulated depolarization times) using the EK and A-P models, respectively. A small difference (i.e., mean error for all vertices <5 ms) and a very good correlation coefficient (0.92) was found between the simulated isochrones predicted by A-P model vs. the EK model. Note that all quantitative comparisons were performed using in-house tools developed in Matlab.

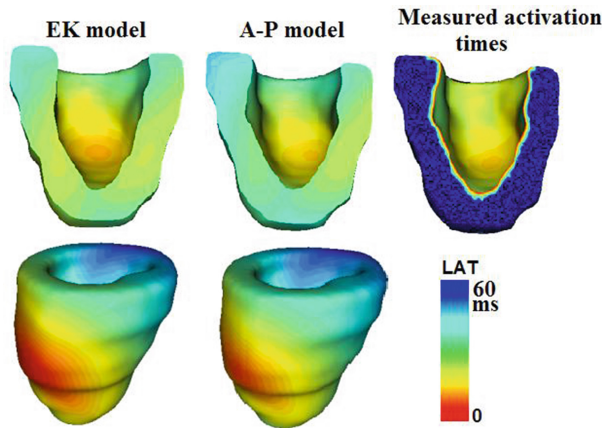


Fig. 5. Comparison between simulated and measured isochrones for the healthy heart (see text for details). For the color scale, red represents the early activation time (EAT), while in blue are late activation times, LAT (ms). In the epicardial maps, EAT corresponded to the location of pacing catheter tip in the MR image. (Color figure online)

Figure 6 shows the results obtained in an infarcted heart (i.e., the same one presented in Fig. 4). The generated mesh had approximately 122 K elements. The simulations with A-P model were performed in <3 min, while the E-K simulations in 18 s (with a time-step of 1×10^{-4} s). For simplicity, we included below only the comparison between the A-P model and experimental isochrones (the latter being projected and interpolated on the endocardial mesh). Overall, there was a good correspondence between of the activation patterns between the maps. The absolute error between the simulated vs. measured endocardial values was 14 ms, which was larger than the error obtained in the healthy case. This can be explained by the fact that the endocardial measurements are sparse (e.g. <60 points), leading to small differences in the activation times within in the peri-infarct areas and adjacent zones, compared to the values computed on 3D meshes.

Overall, the 3D models give superior information compared to the surfacic EP measurements, since they allow visualization of transmural activation times and resulting activation pattern through the myocardial wall, relative to the precise position of the scar in the infarcted hearts.

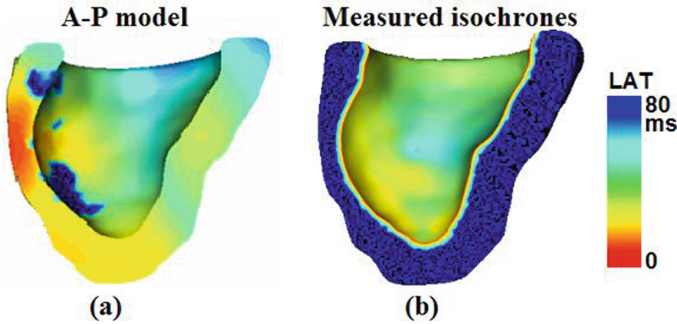


Fig. 6. Comparison between simulated (A-P model) and measured isochrones in one infarcted heart (see text for details).

4 Conclusion and Future Work

Non-invasive evaluation methods of myocardial infarct, such as cardiac MR imaging and predictive image-based computer models can be integrated to provide powerful tools for the clinicians, particularly in EP labs. Such integrative tools can be also used for surgical training [14]. In this work, we proposed a novel framework to augment the information from real-time MR image-guided EP studies with 3D simulations using high-resolution T1-mapping-based computer models. These models could supplement important information that is currently lacking during catheter-based EP procedures due to the sparse and surfacic nature of endocardial electrical maps.

Our preclinical results suggest that macroscopic theoretical models such as A-P and EK can provide very fast simulation results (in <3 min for A-P model, and <20 s for EK model, respectively) for relatively dense MR-based heart meshes, making them

attractive for a rapid integration into the clinical platforms. Although these preliminary results are promising, we acknowledge that a modelling limitation was the usage of *global* parameters (i.e., same conductivity or speed within the healthy tissue of LV). Likely better predictions can be obtained if these key parameters in the A-P and EK models will be calibrated directly from measured EP maps and using the *local* 17-segment AHA model for LV.

Future work will focus on personalizing *local* model parameters per individual heart from EP data as in [15]. We envision that such refined approach will improve the model personalization, particularly in pathological hearts with structural disease. This will enable more accurate predictions of activation maps and, later, an improved outcome of MR-guided EP ablation of scar-related VT patients. Furthermore, for both rapid scar/GZ imaging and image-based model generation, we will use our newly developed high resolution 3D MCLE scan based on a reconstruction method using compressed sensing [16], which will avoid cardiac motion and respiratory registration errors.

Acknowledgement. The authors are grateful for funding and support received from the CIHR, FedDev and Imricor Medical Systems.

References

1. Stevenson, W.G.: Ventricular scars and VT tachycardia. *Trans. Am. Clin. Assoc.* **120**, 403–412 (2009)
2. Bello, D., Fieno, D.S., Kim, R.J., et al.: Infarct morphology identifies patients with substrate for sustained ventricular tachycardia. *J. Am. College Cardiol.* **45**(7), 1104–1108 (2005)
3. Codreanu, A., Odille, F., et al.: Electro-anatomic characterization of post-infarct scars comparison with 3D myocardial scar reconstruction based on MRI. *J. Am. Coll. Cardiol.* **52**, 839–842 (2008)
4. Wijnmaalen, A., van der Geest, R., van Huls van Taxis, C., Siebelink, H., Kroft, L., Bax, J., Reiber, J., Schalij, M., et al.: Head-to-head comparison of c-e MRI and electroanatomical voltage mapping to assess post-infarct scar characteristics in patients with VT: real-time image integration and reversed registration. *Eur. Heart J.* **32**, 104 (2011)
5. Lardo, A.C., McVeigh, E.R., et al.: Visualization and temporal/spatial characterization of cardiac RF ablation lesions using MRI. *Circulation* **102**(6), 698–705 (2000)
6. Oduneye, S.O., Biswas, L., Ghate, S., Ramanan, V., Barry, J., Laish-Farkash, A., Kadmon, E., Zeidan Shwiri, T., Crystal, E., Wright, G.A.: The feasibility of endocardial propagation mapping using MR guidance in a swine model and comparison with standard electro-anatomical mapping. *IEEE Trans. Med. Imaging* **31**(4), 977–983 (2012)
7. Clayton, R.H., Panfilov, A.V.: A guide to modelling cardiac electrical activity in anatomically detailed ventricles. *Progr. Biophys. Mol. Biol. Rev.* **96**(1–3), 19–43 (2008)
8. Pop, M., Ramanan, V., Yang, F., Zhang, L., Newbigging, S., Wright, G.: High resolution 3D T1* mapping and quantitative image analysis of the gray zone in chronic fibrosis. *IEEE Trans. Biomed. Eng.* **61**(12), 2930–2938 (2014)

9. Pop, M., Sermesant, M., Flor, R., Pierre, C., Mansi, T., Oduneye, S., Barry, J., Coudiere, Y., Crystal, E., Ayache, N., Wright, Graham, A.: *In vivo* contact EP data and *ex vivo* MR-based computer models: registration and model-dependent errors. In: Camara, O., Mansi, T., Pop, M., Rhode, K., Sermesant, M., Young, A. (eds.) STACOM 2012. LNCS, vol. 7746, pp. 364–374. Springer, Heidelberg (2013). doi:[10.1007/978-3-642-36961-2_41](https://doi.org/10.1007/978-3-642-36961-2_41)
10. Sermesant, M., Delingette, H., Ayache, N.: An electromechanical model of the heart for image analysis and simulations. *IEEE Trans. Med. Imaging* **25**(5), 612–625 (2006)
11. Aliev, R., Panfilov, A.V.: A simple two variables model of cardiac excitation. *Chaos, Soliton Fractals* **7**(3), 293–301 (1996)
12. Nash, M.P., Panfilov, A.V.: Electromechanical model of excitable tissue to study reentrant cardiac arrhythmias. *Prog. Biophys. Mol. Biol.* **85**, 501–522 (2004)
13. Keener, J.P., Sneyd, J.: *Mathematical Physiology*. Spinger, New York (1998)
14. Talbot, H., Duriez, C., Courtecuisse, H., Relan, J., Sermesant, M., Cotin, S., Delingette, H.: Towards real-time computation of cardiac electrophysiology for training simulator. In: Camara, O., Mansi, T., Pop, M., Rhode, K., Sermesant, M., Young, A. (eds.) STACOM 2012. LNCS, vol. 7746, pp. 298–306. Springer, Heidelberg (2013). doi:[10.1007/978-3-642-36961-2_34](https://doi.org/10.1007/978-3-642-36961-2_34)
15. Chinchapatnam, P., Rhode, K.S., Ginks, M., et al.: Model-based imaging of cardiac apparent conductivity and local conduction velocity for planning of therapy. *IEEE Trans. Med. Imaging* **27**(11), 1631–1642 (2008)
16. Li, Z., Athavale, P., Pop, M., Wright, G.A.: Multi-contrast reconstruction using compressed sensing with low rank and spatially-varying edge-preserving constraints for high-resolution MR characterization of myocardial infarction. *Magn. Reson. Med.* (September 2016, in press (Pubmed)). doi:[10.1002/mrm.26402](https://doi.org/10.1002/mrm.26402)

Statistical Atlases and Computational Models of the
Heart. Imaging and Modelling Challenges
7th International Workshop, STACOM 2016, Held in
Conjunction with MICCAI 2016, Athens, Greece, October
17, 2016, Revised Selected Papers
Mansi, T.; McLeod, K.; Pop, M.; Rhode, K.; Sermesant,
M.; Young, A. (Eds.)
2017, XI, 230 p. 108 illus., Softcover
ISBN: 978-3-319-52717-8